Polarization Singularities from Unfolding an Optical Vortex through a Birefringent Crystal

Florian Flossmann, Ulrich T. Schwarz,* and Max Maier

Naturwissenschaftliche Fakultät II-Physik, Universität Regensburg, Universitätsstraße 31, D-93053 Regensburg, Germany

Mark R. Dennis

School of Mathematics, University of Southampton, Highfield, Southampton SO17 1BJ, United Kingdom
(Received 9 August 2005; published 12 December 2005)

Optical vortices (nodal lines and phase singularities) are the generic singularities of scalar optics but are unstable in vector optics. We investigate experimentally and theoretically the unfolding of a uniformly polarized optical vortex beam on propagation through a birefringent crystal and characterize the output field in terms of polarization singularities (C lines and points of circular polarization; L surfaces and lines of linear polarization). The field is described both in the 2-dimensional transverse plane, and in three dimensions, where the third is abstract, representing an optical path length propagated through the crystal. Many phenomena of singular optics, such as topological charge conservation and singularity reconnections, occur naturally in the description.

Topological defects are of significance in wave physics because of their stability and persistence upon propagation in time or space [1,2]. This stability is due to their local structure, which organizes the topology of the surrounding field, and depends delicately on the symmetries of the system. In optical beams, different quantities often have different symmetries: when beams carry both orbital and spin angular momentum (as is the case with the rotational Doppler effect [3]), the total field intensity has cylindrical symmetry, but the polarization does not.

Here, we investigate the generic unfolding of the natural defects of scalar optics, namely, optical vortices (also called phase singularities, nodal lines, or wave dislocations) [2], when a light beam propagates through a birefringent crystal. The uniform polarization of the incident beam is resolved into the two orthogonal linear polarizations according to the crystal's birefringence, which propagate in different directions due to extraordinary refraction. The resulting interference of the two waves gives rise to a complicated space-dependent polarization pattern, which we characterize in terms of the generic singularities of polarization optics, namely, L surfaces where the polarization is linear and C lines where the polarization is circular [2,4,5]. These singularities intersect the transverse plane of observation along L lines and C points, respectively.

Optical vortex lines are significant throughout optics, in polarized components of the electromagnetic field. They are places where the complex scalar amplitude describing the field is zero, and the phase change around the vortex is quantized in integer units (positive or negative) of 2π ("charge") [2]. Examples are vortices in laser beams, which can be tightly controlled by holograms, such as in the creation of vortex knots and braids [6,7], as well as naturally tangling in random speckle patterns [8]. Optical vortices often studied in laser beams carry orbital angular momentum (see, e.g., Refs. [2,3,9]) and are equivalent to quantized vortices in Bose-Einstein condensates [10],

superconductors, and superfluids [11]. Polarization singularities occur in fields where the state of (generally elliptic) transverse polarization varies with position. L lines and surfaces separate regions of opposite handedness [2], and C lines and points are characterized by a disclination index $\pm 1/2$, analogous to defects in nematic liquid crystals [2,12]. These singularities occur naturally in polarization speckle fields [5,13], near field micro-optics [14], and skylight [15]. Polarization singularities in crystal optics have been investigated previously [16,17], although apparently not with incident beams containing vortices.

We find, when a monochromatic, uniformly polarized light beam with an embedded optical vortex propagates through a birefringent crystal, that the emerging field's polarization has a network of singularities with a simple, universal structure: a double helix of C lines, and an L surface topologically equivalent to Riemann's periodic minimal surface. This structure is 3 dimensional; in addition to transverse *x, y* structure of the emerging field, there is an abstract third dimension given by optical path length propagated through the crystal, determining the phase shift between the two crystal eigenpolarizations. The physical origin of the effect is explained due to interference of these eigenpolarizations, and the pattern is explored and verified experimentally.

The incident field is $\mathbf{E}_{in}(x, y) = \psi(x, y)\mathbf{d}_{in}$, where the 2-dimensional complex vector $\mathbf{d}_{in}$ represents a uniform, possibly elliptic state of transverse polarization, and the complex scalar $\psi(x, y)$ is the amplitude. In the direction of propagation *z*, a transparent nonchiral crystal has two orthogonal linear eigenpolarizations $\mathbf{d}_1, \mathbf{d}_2$ with refractive indices n_1, n_2, distinct when away from the optic axes of the crystal (whether uniaxial or biaxial). $\mathbf{E}_{in}$ is resolved into the two crystal eigenpolarizations which are refracted appropriately, resulting, in the emerging beam, in a spatial shift $\pm s_j$ (assumed to be in the *x* direction), including beam walk-off for the extraordinary beam(s). A relative

phase shift Λ, dependent on $n_2 - n_1$ times the distance, is accumulated during propagation through the crystal. These three effects give an emerging polarization pattern of the form

$$\mathbf{E}(x, y, \Lambda) = \sum_{j=1,2} \psi(x + s_j, y)(\mathbf{d}_{\text{in}} \cdot \mathbf{d}_j)\mathbf{d}_j e^{i(-1)^j \Lambda/2} \quad (1)$$

up to an unimportant spatial translation. We are interested in the case when ψ contains a singly quantized vortex, such as a Laguerre-Gauss LG_0^1 beam, represented in the focal plane by

$$\psi_{LG_0^1}(x, y) = (x + iy)\exp[-(x^2 + y^2)/w_0^2] \quad (2)$$

(w_0 is the waist width). For an elliptically polarized incident beam, $\mathbf{d}_{\text{in}}$ can be written $\mathbf{d}_1 \cos\beta + \mathbf{d}_2 \sin\beta e^{i\delta}$, with ellipticity $\varepsilon = \sin2\beta \sin\delta$ [see Fig. 1(a)]. From (1), $\delta \neq 0$ results merely in a constant phase shift to the second term, so we need only to consider $\mathbf{d}_{\text{in}}$ linearly polarized, $\mathbf{d}_{\text{in}} = \mathbf{d}_1 \cos\alpha_{\text{in}} + \mathbf{d}_2 \sin\alpha_{\text{in}}$.

In our experiment, a linearly polarized LG_0^1 beam propagates through a uniaxial crystal, with the optic axis in the (x, z) plane [see Fig. 1(b)]. The topological agreement between the experiment and model (1) is sufficiently close that the physical discussion can be illustrated using experimental results.

Our experimental setup is represented in Fig. 1(c). A Laguerre-Gauss beam $\psi_{LG_0^1}$ with uniform linear polarization $\mathbf{d}_{\text{in}}$ is synthesized from a He-Ne beam, using a polarizer and spatial light modulator (SLM). Higher diffraction orders from the SLM are removed by a telescope and a pinhole. The KDP birefringent crystal is located
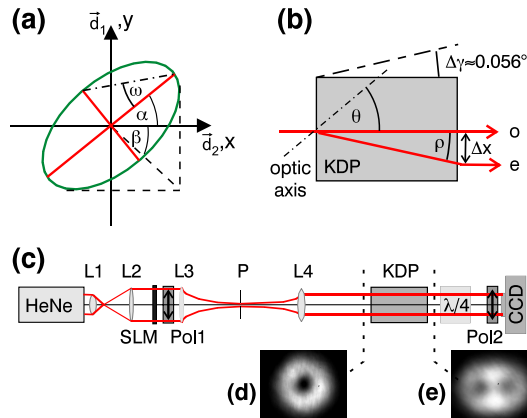

FIG. 1 (color online). (a) Definition of ellipse parameters [cf. Eqs. (4) and (5)]: α is the angle of the major axis, $\tan\beta$ is the ratio of the y and x components of the field, and the ellipticity is $\varepsilon = \sin2\omega$; (b) orientation of a uniaxial crystal, and ordinary and extraordinary rays (angles are exaggerated); (c) experimental setup scheme (HeNe: laser; SLM: spatial light modulator; L1 ··· L4: lenses; P: pinhole; KDP (potassium dihydrogen phosphate): birefringent crystal; Pol1, Pol2: linear polarizer/analyzer; $\lambda/4$ plate; CCD: camera). Insets (d) and (e) show the total intensity distribution before and after the birefringent crystal, respectively.

in the waist plane, where ψ has the form (2) with $w_0 = 0.7$ mm. Because of the large Rayleigh range ($z_R \approx 2.4$ m), phase front curvature, Gouy phase shift, and diffraction can be neglected over the change of optical path length relevant for the effects we describe.

Our sample of uniaxial KDP has dimensions $x \times y \times z = 20 \times 20 \times 26$ mm^2 cut at $40°$ to the optic axis. In our experiment, the incoming beam is at normal incidence. The ordinary polarization $\mathbf{d}_1$ is $(0, 1)$, the extraordinary polarization $\mathbf{d}_2 = (1, 0)$. The relative phase shift is

$$\Lambda = 2\pi(n_2 - n_1)l/\lambda_{\text{vac}}. \quad (3)$$

Here $n_1 = n_0 = 1.507$ for the ordinary and $n_2 = n(\theta = 40°) = 1.490$ for the extraordinary beam. We vary Λ experimentally by rotating the crystal about the y axis, which does not change $\mathbf{d}_{1,2}$; one Λ period corresponds to $\Delta\gamma = 0.056°$ [see Fig. 1(b)]. The optical path length changes due to the change in $n(\theta)$; the change in geometric path length l is negligible. We measure the outgoing Stokes parameters at 75 positions equally spaced through $\Lambda = 0 \cdots 4\pi$. The relative transverse shift $\Delta x = s_2 - s_1 = 0.7$ mm is determined by the walk-off angle $\rho = \theta' - \theta = 1.52°$, where θ is the angle of normal velocity with respect to the optic axis, and θ' is the angle of the ray velocity. For the small rotation $\Delta\gamma$ the transverse shift Δx is effectively constant. The field emerging from the crystal can therefore be approximated by Eq. (1) for a range of Λ.

For each (x, y, Λ), the four Stokes parameters $S_0 \cdots S_3$ describing the polarization state are reconstructed from seven intensity measurements by a CCD camera with different combinations of a polarizer and a $\lambda/4$ plate [18]. The geometric quantities (angle α and ellipticity ε) of the elliptic polarization state are determined by

$$\alpha = \tfrac{1}{2}\arg(S_1 + iS_2)$$
$$= \tfrac{1}{2}\arg\{(I_{90°} - I_{0°}) + i(I_{45°} - I_{135°})\}, \quad (4)$$

$$\varepsilon = S_3/S_0 = (I_{\text{RCP}} - I_{\text{LCP}})/S_0. \quad (5)$$

The subscript of I denotes the orientation of the analyzer and right- and left-handed circular polarization, RCP and LCP, determined using a $\lambda/4$ plate. We will describe the (x, y, Λ) configuration of the emerging polarization field, which is further parametrized by the state $\mathbf{d}_{\text{in}}$ of initial polarization. We begin by describing the 2-dimensional field for a fixed constant Λ.

We plot the intensity and polarization of a typical transverse plane of the emerging field, with phase shift $\Lambda_0 = 0.9\pi$ and linear input polarization $\alpha_{\text{in}} = 40°$, in Fig. 2. Unlike the incident beam, the intensity vanishes nowhere, although there are minima near the zeros in the two shifted components. There are four isolated C points, and a closed loop L line, which encloses a region of right-handed elliptic polarization (the elliptic polarization in the rest of the figure is left-handed). The C points are marked by colored circles which correspond to the 3-dimensional C lines, discussed later in Fig. 4. The original vortex is refracted
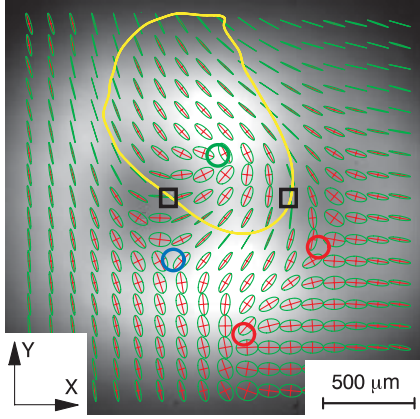
FIG. 2 (color). Intensity and polarization in the x, y plane of the output field **E**, for an arbitrary choice $\Lambda = \Lambda_0 = 0.9\pi$. The input beam is linearly polarized at $\alpha_{in} = 40°$. Polarization ellipses and axes are superimposed, plotted with major axes normalized. The four C points of circular polarization are marked by colored circles, and the L line loop of linear polarization is represented by a solid yellow line. Polarization is left-handed except within the L loop, where it is right-handed. The black squares are the positions of the original vortex after double refraction.

FIG. 3 (color). Two equivalent representations of the measured polarization angle α, for the case plotted in Fig. 2. (a) Contour plot of α; black curves are isogyres; (b) polarization streamlines (α is the curve tangent angle). The upper and lower C points are lemon-type, with index $+1/2$, the two on the left and right are stars, with index $-1/2$. The L line is shown in yellow, and black squares mark the positions of the doubly refracted original vortex.

differently in the two components, emerging at the two points (black squares) on the L line where the polarization is purely parallel to $\mathbf{d}_1$ and $\mathbf{d}_2$. Since the central vortex is the only zero in $\psi_{\mathbf{LG}_0^1}$, from (2), these are the only points on the L line loop with these polarization angles.

The singular nature of C points is emphasized in Fig. 3(a), where isogyres (contours of constant α) are plotted. These isogyres end on the C points (where α is not defined), and the $\pm$ sense of α increase about the C point determines its index, $\pm 1/2$ [4,5]. This index's half-integer nature is due to the π-rotational symmetry of a (noncircular) ellipse, analogous to liquid crystal disclination defects [12]. In Figs. 2 and 3, the upper and lower C points (including the right-handed one) have index $+1/2$, the others $-1/2$. The geometry of the α pattern is plotted in Fig. 3(b), as a set of polarization streamlines. Here, the tangent to the curve through a point is the direction of α. The two $+1/2$ C points have a "lemon"-like geometry, the $-1/2$ points have 3-fold "star" structure [2,4,5].

The total index of the C points of **E** in Figs. 2 and 3 agrees with the total topological charge of the incoming (scalar) field $\mathbf{E}_{in} = \psi\mathbf{d}_{in}$, as expected in the unfolding of a topological singularity. This can be seen using the complex polarization scalar $\varphi = \mathbf{E} \cdot \mathbf{E}$, which contains both polarization and phase information [5,19]. φ has phase singularities at the C points of **E**, with (integer) charge equal to the disclination index sign times the handedness sign ($+$ for right-handed, $-$ for left-handed). Evidently, φ of the field in Figs. 2 and 3 has 3 positive singularities (one right-handed lemon and two left-handed stars) and one negative singularity [one left-handed lemon; lower red circle in Fig. 3(b)]: the net topological charge is $+2$. For the in-
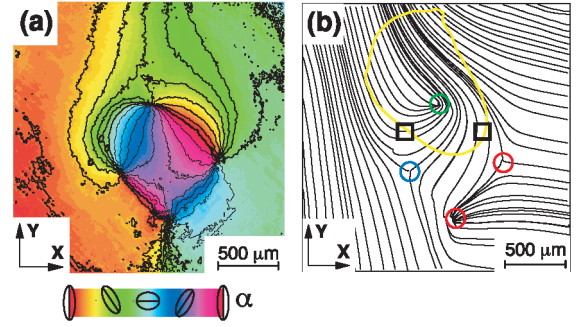
coming field, $\varphi_{in} = \mathbf{E}_{in} \cdot \mathbf{E}_{in} = \psi^2 \mathbf{d}_{in} \cdot \mathbf{d}_{in}$ also has a charge of $+2$ (provided the incoming polarization is not circular); topological charge is preserved as the beam propagates through the crystal.

The effect on the fields of Figs. 2 and 3 of increasing Λ by π (i.e., $\Lambda = \Lambda_0 + \pi$) is equivalent to the action of a $\lambda/2$ plate: $\varepsilon \to -\varepsilon$ (handedness reversed) and $\alpha \to -\alpha$. Thus, in the $\Lambda_0 + \pi$ plane, C points have the same (x, y) coordinates, but opposite handedness and disclination index. The total vector field singularity index (handedness times index, summed over the C points) is unchanged.

Properties of the full 3-dimensional structure can be inferred from these observations. C lines and L surfaces measured over a range of $\Lambda = 0 \cdots 4\pi$ for the input polarizations $\alpha_{in} = 40°$ (as in Figs. 2 and 3) and $\alpha_{in} = 45°$ are plotted in Figs. 4(a) and 4(b). For typical fixed Λ (as in Figs. 2 and 3), there is a dominant polarization handedness. However, after half a Λ period, this dominant handedness must change, leading to alternating handedness layers. The presence of the C point in the island of right-handed polarization in Fig. 2, corresponding to the green line in Fig. 4(a), implies that layers of the same handedness are connected. The polarization at the points corresponding to the refracted vortex in the two waves [i.e., $y = 0$ and $x = s_j$ in (1)] is linear for all Λ. In (x, y, Λ) space, volumes of opposite handedness are separated by a single, connected L surface (see Fig. 4). This L surface is structurally stable and topologically equivalent to Riemann's periodic minimal surface [20].

Because of the conserved topological charge of 2 and the earlier observations, there are evidently two continuous C lines of opposite disclination index and handedness threading through the periodic structure, as shown by the blue and green lines in Fig. 4(a). The $\lambda/2$ symmetry in Λ implies that the C lines coil around each other in a double helix. The other two C points (red circles) of Fig. 2, with the same handedness but opposite index, lie on the same C
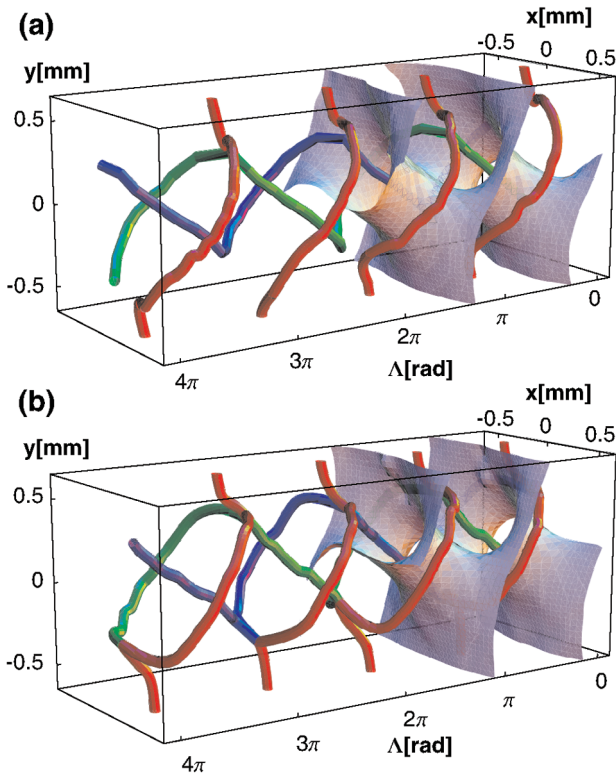
FIG. 4 (color). Experimentally determined configuration of polarization singularities (L surface and C lines) in (x, y, Λ) space for input polarizations (a) $\alpha_{in} = 40°$ and (b) $\alpha_{in} = 45°$. Λ increases from 0 to 4π, the L surface is plotted from 0 to 2π. In (a) all C lines are disconnected; in (b) reconnections occur.

line which intersects the Λ_0 plane twice. This C line is confined to that handedness layer: this does not thread through the structure and does not increase monotonically with Λ, but extends to $\pm\infty$ in the y direction. There are regions of Λ where this C line does not intersect the transverse plane.

The sense of twist of the C line double helix is determined by which of $\mathbf{d}_{1,2}$ the incident $\mathbf{d}_{in}$ is closer to; it switches when $\alpha_{in} = 45°$. As α_{in} approaches this symmetric configuration, two pairs of C lines of the same handedness approach at intervals of π in Λ, and reconnections occur at $\alpha_{in} = 45°$; such topological reactions occur stably in three dimensions as a fourth parameter is varied [7,9,21]. The symmetric configuration with reconnections is shown in Fig. 4(b). The topology of the C lines in the symmetric and nonsymmetric arrangements is reminiscent of the braided vortices construction of Ref. [7]. That specific superposition shares some similarity to what occurs here naturally; however, there are only two coiled C lines here, rather than three necessary to form a braid.

We have described in detail the 2- and 3-dimensional topological structure of the polarization singularities of a scalar vortex beam propagated through a birefringent crystal. The physical origin of the structure has been described, and the features have been observed and illustrated experimentally. Many features of singular optics (e.g., conservation of topological index, stability of structures, and reconnections) occur naturally in this simple physical situation, showing the topological interplay between scalar and vector optics. The polarization singularity structure would be more complicated through a more complicated crystal (with optical activity and dichroism), or with nonmonochromatic light [16].

*Electronic address: ulrich.schwarz@physik.uni-r.de

[1] J. F. Nye and M. V. Berry, Proc. R. Soc. A **336**, 165 (1974).
[2] J. F. Nye, *Natural Focusing and Fine Structure of Light* (Institute of Physics Publishing, Bristol, 1999).
[3] J. Courtial, D. A. Robertson, K. Dholakia, L. Allen, and M. J. Padgett, Phys. Rev. Lett. **81**, 4828 (1998).
[4] J. F. Nye, Proc. R. Soc. A **389**, 279 (1983).
[5] M. R. Dennis, Opt. Commun. **213**, 201 (2002).
[6] J. Leach, M. R. Dennis, J. Courtial, and M. J. Padgett, Nature (London) **432**, 165 (2004).
[7] M. R. Dennis, New J. Phys. **5**, 134 (2003).
[8] M. V. Berry and M. R. Dennis, Proc. R. Soc. A **456**, 2059 (2000).
[9] G. Molina-Terriza, J. Recolons, J. P. Torres, L. Torner, and E. M. Wright, Phys. Rev. Lett. **87**, 023902 (2001).
[10] M. R. Matthews, B. P. Anderson, P. C. Haljan, D. S. Hall, C. E. Wieman, and E. A. Cornell, Phys. Rev. Lett. **83**, 2498 (1999).
[11] R. P. Feynman, in *Progress in Low Temperature Physics*, edited by C. J. Gorter (North-Holland, Amsterdam, 1955), Vol. 1, p. 17.
[12] P. G. de Gennes and J. Prost, *The Physics of Liquid Crystals* (Oxford University Press, New York, 1993).
[13] M. Soskin, V. Denisenko, and R. Egorov, J. Opt. A **6**, S281 (2004).
[14] A. Nesci, R. Dändliker, M. Salt, and H. P. Herzig, Opt. Commun. **205**, 229 (2002).
[15] M. V. Berry, M. R. Dennis, and R. L. Lee, New J. Phys. **6**, 162 (2004).
[16] Y. A. Egorov, T. A. Fadeyeva, and A. V. Volyar, J. Opt. A **6**, S217 (2004); A. V. Volyar and T. A. Fadeyeva, Tech. Phys. Lett. **29**, 111 (2003).
[17] M. V. Berry and M. R. Dennis, Proc. R. Soc. A **459**, 1261 (2003).
[18] D. S. Kliger, J. W. Lewis, and C. E. Randall, *Polarized Light in Optics and Spectroscopy* (Academic Press, Boston, 1990).
[19] M. V. Berry and M. R. Dennis, Proc. R. Soc. A **457**, 141 (2001).
[20] B. Riemann, in *Bernhard Riemann's Gesammelte Mathematische Werke und Wissenschaftlicher Nachlass*, edited by H. Weber (Teubner, Leipzig, 1892), p. 301.
[21] J. F. Nye, J. Opt. A **6**, S251 (2004).